ELECTRON BEAM SIZE MEASUREMENTS USING THE HETERODYNE NEAR FIELD SPECKLES AT ALBA

M. Siano*, B. Paroli, M. A. C. Potenza, Università degli Studi di Milano, 20133 Milan, Italy
U. Iriso, C. S. Kamma-Lorger, A. A. Nosych, ALBA, Cerdanyola del Valles, Barcelona, Spain
S. Mazzoni, G. Trad, CERN, Geneva, Switzerland

Abstract

Experiments using the Heterodyne Near Field Speckle method (HNFS) have been performed at ALBA to characterize the spatial coherence of the synchrotron radiation, with the ultimate goal of measuring both the horizontal and vertical electron beam sizes. The HNFS technique consists on the analysis of the interference between the radiation scattered by a colloidal suspension of nanoparticles and the synchrotron radiation, which in this case corresponds to the hard X-rays (12 keV) produced by the in-vacuum undulator of the NCD-Sweet beamline. This paper describes the fundamentals of the technique, possible limitations, and shows the first experimental results changing the beam coupling of the storage ring.

INTRODUCTION

At the ALBA storage ring, beam size monitoring is routinely performed by means of an X-ray pinhole camera [1]. Furthermore, parallel reliable measurements are provided by Young interferometry with visible synchrotron radiation [2,3]. A novel and unconventional interferometric beam size measurement technique is offered by the Heterodyne Near Field Speckle method (HNFS). It relies on the statistical analysis of the speckled intensity distribution generated by calibrated spherical nanoparticles of known properties enlightened by the Synchrotron Radiation (SR) extracted from the accelerator. It was developed almost twenty years ago at optical wavelengths as a particle sizing technique [4,5] and then extended to the X-ray region of the spectrum [6]. More recently it has found applications in accelerator beam instrumentation [7–10] allowing to probe the SR two-dimensional (2D) transverse coherence described by the Complex Coherence Factor (CCF) [11,12]:

$$\mu(\Delta\vec{r}) = \frac{\langle E(\vec{r})E^*(\vec{r} + \Delta\vec{r})\rangle}{\sqrt{\langle I(\vec{r})\rangle \langle I(\vec{r} + \Delta\vec{r})\rangle}} \quad . \tag{1}$$

In Eq. (1), E is the electric field, $I = \langle|E|^2\rangle$ is the associated intensity, $\vec{r} = (x, y)$ denotes transverse position on a x-y plane perpendicular to the propagation direction, and finally $\langle\cdots\rangle$ denotes ensemble averages. Under the conditions of validity of the Van Cittert and Zernike (VCZ) theorem [11,12], the 2D transverse profile of the electron beam can then be retrieved from the measured 2D CCF.

We report here a proof of concept experiment for two dimensional beam size measurement using the 12 keV hard X-rays produced at the NCD-Sweet beamline at ALBA. The paper is organized as follows: after briefly reviewing the

fundamentals of the HNFS method, we describe the NCD-Sweet beamline and the experimental setup therein installed; then we show and discuss the first results obtained by changing the coupling in the storage ring; finally, we collect our conclusions.

THE HNFS TECHNIQUE

The HNFS technique relies on the self-referencing interference between the spherical waves scattered by the particles of the colloidal suspension and the transilluminating field. For a single scattering particle, the interference image is composed by circular fringes whose visibility is reduced according to the 2D CCF of the incoming radiation at the scattering plane. An example is shown in Fig. 1(a) where results of numerical simulations are reported for the case of incoming radiation endowed with larger coherence along the vertical direction to mimic the case typically encountered in undulator beamlines. The random superposition on an intensity basis of many of these single-particle interferograms results in a stochastic intensity distribution known as heterodyne speckle field, as shown in Figs. 1(b) and (c).
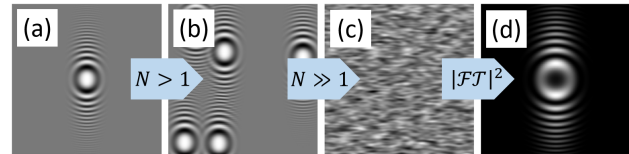

Figure 1: Fundamentals of the HNFS technique. (a) Single-particle interferogram for incoming radiation with larger coherence along the vertical direction. (b) and (c) The random sum of many single-particle interferograms generates a so-called speckle field. (d) The 2D power spectrum of heterodyne speckles allows to retrieve the interferometric information on coherence conveyed by the single-particle interference image.

Coherence information is retrieved by Fourier analysis of the speckle field – Fig. 1(d). In fact, the 2D power spectrum closely resembles the single-particle interferogram. It exhibits peculiar oscillations (Talbot oscillations) enveloped by the squared modulus of the radiation CCF [7–10]:

$$I(\vec{q}, z) = |\mu[\Delta\vec{r}(\vec{q}, z)]|^2 T(q, z) \quad , \tag{2}$$

where $I(\vec{q}, z)$ is the 2D spatial power spectrum of heterodyne speckles at a distance z from the scattering plane, $T(q, z) = 2\sin^2[zq^2/(2k)]$ is known as the Talbot Transfer Function (TTF), $\vec{q}$ is the Fourier wavevector, $q = |\vec{q}|$, $k = 2\pi/\lambda$ where λ is the radiation wavelength, and finally

$$\Delta\vec{r}(\vec{q}, z) = z\frac{\vec{q}}{k} \quad . \tag{3}$$

Equation 3 is known as the spatial scaling of the HNFS technique [7–10] and it allows to probe the SR CCF from measurements of the power spectrum as a function of transverse displacements. It is worth noticing how larger z allows better sampling of the radiation CCF in the transverse plane, thus being more suitable in presence of higher coherence properties. From the 2D power spectrum, profiles along given directions can be extracted. To reduce noise, angular average within narrow angular sectors can be also obtained, as depicted in Fig. 2 (a).
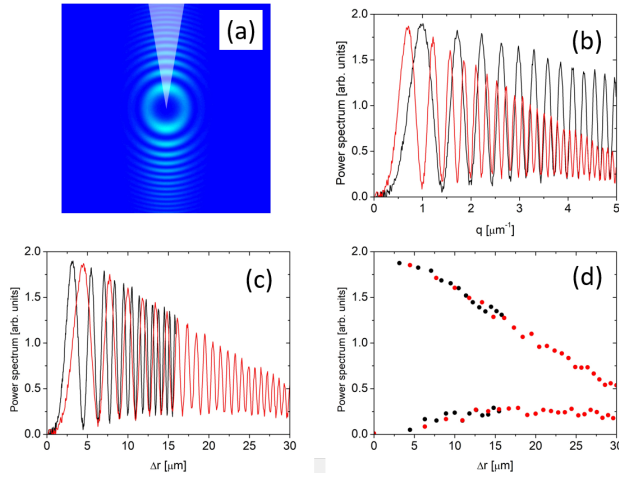

Figure 2: Example of data reduction and visualization. (a) Simulated 2D power spectrum. Vertical profiles are obtained as averages within the highlighted angular sector. (b) Talbot oscillations at two different distances fail to describe a unique master curve when plotted as a function of Fourier wavevectors. (c) The same profiles fulfill the spatial master curve criterion upon the spatial scaling. (d) Upper and lower envelopes identified by Talbot maxima and minima, respectively. The CCF is obtained from their average.

Since the SR CCF is probed at the scattering plane, data obtained at different z must collapse onto one curve upon the spatial scaling, as shown in Figs. 2(b) and (c). We refer to this phenomenon as the spatial master curve criterion. In particular, we show in Fig. 2(d) how Talbot maxima and minima identify two different unique curves, referred to as the upper and lower envelopes of scaled Talbot oscillations. The radiation CCF is obtained from their average.

EXPERIMENTAL SETUP

The experimental setup installed at the NCD-Sweet beamline is depicted in Fig. 3. The radiation source is an In-Vacuum Undulator (IVU) with period $\lambda_w = 21.3$ mm and 92 periods. A channel cut silicon monochromator selects the photon wavelength $\lambda = 0.1$ nm ($E = 12.4$ keV) with a relative bandwidth $\Delta\lambda/\lambda = 10^{-4}$. The scattering sample is located at $Z^0 = 33$ m from the undulator center. It is composed by an aqueous suspension of silica nanospheres 500 nm in diameter, stored in capillaries of 1.5 mm diameter. Speckles are acquired at a distance z downstream the sample,

with z ranging from 20 mm to 900 mm. Usage of a YAG:Ce scintillator 0.1 mm in thickness to convert the X-ray photons into visible light allows to exploit standard visible optics (20x microscope objective, $N.A. = 0.4$) and CCD cameras (model Basler scA1300-32gm) for image acquisition. For each fixed z, we acquire 50 images at a frame rate of 2 Hz to increase statistics.
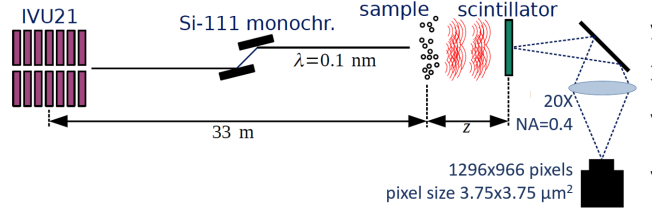

Figure 3: Schematic drawing of the HNFS setup installed at NCD-Sweet beamline at ALBA.

In order to validate the technique, two different sets of measurements are taken: one with the nominal coupling ($\kappa = 0.65\%$, used in standard operation), and a second one in which the beam coupling is increased up to around $\kappa = 2\%$ using the skew quadrupoles. Thus, the beam size at the NCD source point changes for different couplings, as depicted in Fig. 4, especially in the vertical direction (from 6.3 to 10.7 μm at the IVU center - values provided after a LOCO measurement [13]).
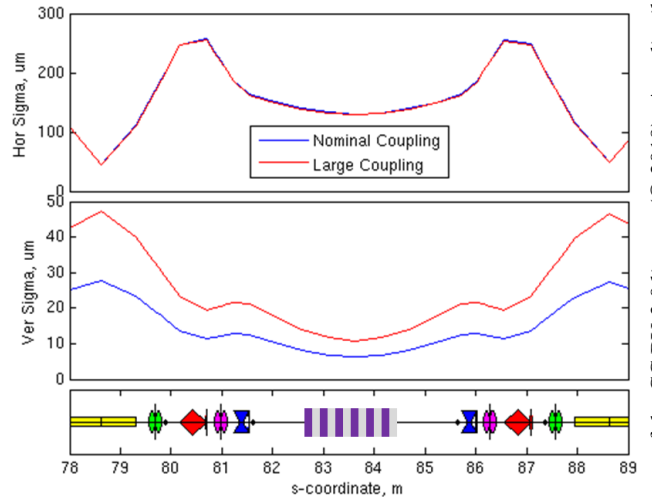

Figure 4: Theoretical evolution of the horizontal (top) and vertical (middle) electron beam sizes around the NCD location for two different couplings.

RESULTS AND DISCUSSION

Scaled horizontal and vertical profiles of power spectra at all the sample-detector distances are presented in Fig. 5 for $\kappa = 0.65\%$ and in Fig. 6 for $\kappa = 2\%$. For the ease of visualization, only Talbot maxima and minima are shown. The squared modulus of the SR CCF is computed from the average between binned Talbot maxima and minima. Data are then fitted to a Gaussian curve to extract a measure of
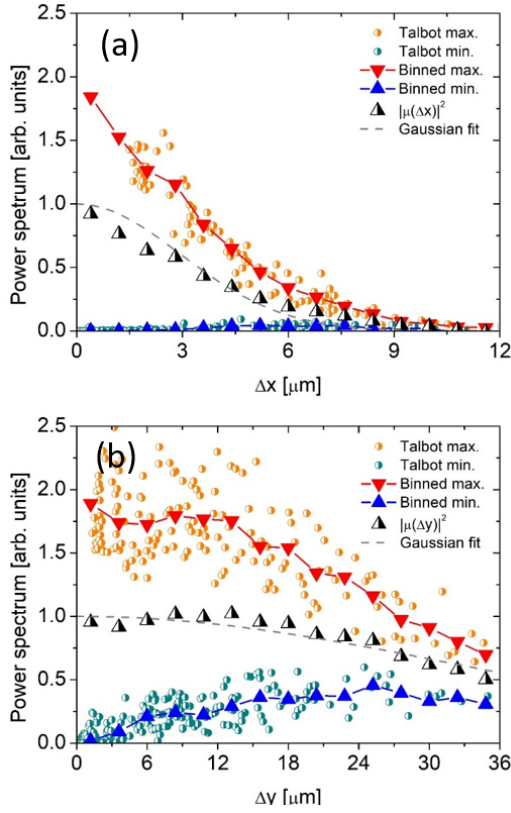
Figure 5: Results for $\kappa = 0.65\%$ along the (a) horizontal and (b) vertical directions.
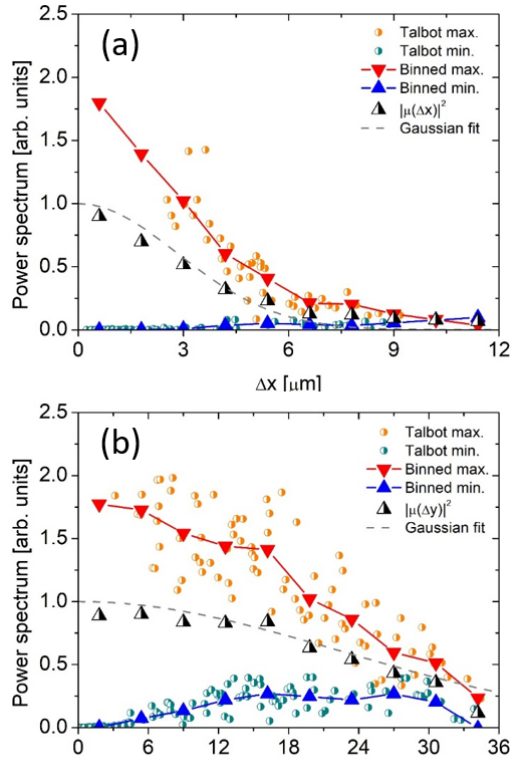

Figure 6: Results for $\kappa = 2\%$ along the (a) horizontal and (b) vertical directions.

the transverse coherence length according to the definition given by Mandel [11, 12]:

$$\sigma_{\text{coh}}^u = \int_{-\infty}^{+\infty} |\mu(\Delta u)|^2 \, \text{d}\Delta u \quad , \qquad (4)$$

with u the general transverse coordinate, x or y. It is worth noticing how the HNFS technique provides a direct measurement of the integrand in Eq. (4), from where we derive the coherence lengths $(\sigma_{\text{coh}}^x, \sigma_{\text{coh}}^y) = (7.4 \pm 0.4, 83 \pm 7)\,\mu\text{m}$ for $\kappa = 0.65\%$, and $(7.1 \pm 0.5, 57 \pm 5)\,\mu\text{m}$ for $\kappa = 2\%$.

From the coherence length, the rms electron beam size in the transverse direction can be retrieved by applying the VCZ theorem:

$$\sigma_u = \frac{\lambda Z^0}{2\sqrt{\pi}\sigma_{\text{coh}}^u} \quad . \qquad (5)$$

For the horizontal case, the inferred beam size agrees well (within the error bars) with the LOCO results (see Table 1).

However, for the very small beam sizes in the vertical case, discrepancies arise as the conditions of validity of the VCZ theorem are not fulfilled [14]. In particular, the radiation source cannot be modelled as quasi-homogeneous, or equivalently as a thermal source [11, 12] and other effects need to be taken into account to compute the coherence length.

We performed simulations based on the formulas in Ref. [14] and including other non-ideal behaviour of the experimental set-up, such as detuning in the radiation wavelength (undulator resonant wavelength at the 7th harmonic is $\lambda_{\text{res}}^{(7)} = 0.0964$ nm at $K = 1.6$) and finite energy spread of the particle beam ($\Delta E/E = 1.05 \cdot 10^{-3}$). Results are shown in Fig. 7 for $\kappa = 0.65\%$ and for $\kappa = 2\%$. The plot shows the evolution of the horizontal and vertical transverse coherence lengths as a function of the distance from the undulator center for an electron beam with sizes as in Fig. 4.
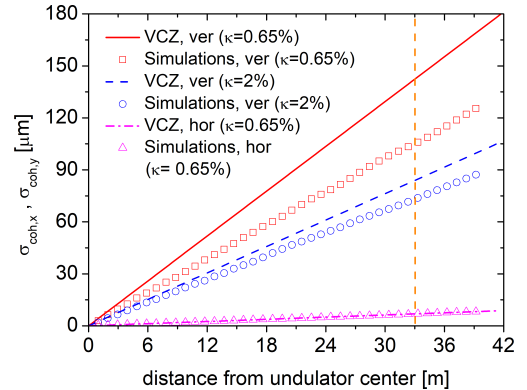

Figure 7: Simulations of horizontal and vertical transverse coherence length as a function of the distance from the undulator center (beam sizes as in Fig. 4). Results for $\kappa = 0.65\%$ and $\kappa = 2\%$ are similar for the horizontal case and only one curve is reported. The vertical line represents the HNFS setup position.

The complete simulations give the same predictions as the VCZ theorem along the horizontal direction, in agreement with the conclusions in Ref. [14] and therefore confirming the reliability of our measurements. As for the vertical case, the VCZ theorem cannot be applied neither for $\kappa = 0.65\%$

nor for $\kappa = 2\%$. In particular, the VCZ predictions are 1.36 times larger for $\kappa = 0.65\%$ and 1.30 times larger for $\kappa = 2\%$. The precise relation between vertical coherence length and beam size is still under investigation and we plan to perform thorough systematic simulations to derive it. As a first approximation we assume that the same correction factor applies to the beam size, therefore yielding $\sigma_y = (8.1 \pm 0.7)\,\mu\text{m}$ for $\kappa = 0.65\%$ and $\sigma_y = (12.5 \pm 1.6)\,\mu\text{m}$ for $\kappa = 2\%$. Table 1 gives the different beam size results according to the different methods to calculate them: VCZ stands for the direct use of the Van Citter and Zernike theorem, SIM refers to the beam size calculations inferred from the coherence lengths simulated in Fig. 7, and LOCO stands for the theoretical calculations inferred from the optics model.

Table 1: Horizontal and vertical measurements of the transverse coherence lengths, and corresponding electron beam sizes inferred from the different methods in the text.

		method	$\kappa = 0.65\%$	$\kappa = 2.0\%$
σ_x^{coh}	[μm]		7.4 ± 0.4	7.1 ± 0.5
σ_x	[μm]	VCZ	125 ± 5	130 ± 10
σ_x	[μm]	SIM	124 ± 5	125 ± 9
σ_x	[μm]	LOCO	130	129
σ_y^{coh}	[μm]		83 ± 7	57 ± 5
σ_y	[μm]	VCZ	11 ± 1	16 ± 2
σ_y	[μm]	SIM	8.1 ± 0.7	12.5 ± 1.6
σ_y	[μm]	LOCO	6.3	10.7

CONCLUSIONS

We have performed a proof of principle experiment at the NCD-Sweet beamline at ALBA to test the HNFS method as a 2D beam size measurement technique. By changing the beam coupling, two different values of the beam sizes have been probed: $(130, 6.3)\,\mu\text{m}$ for $\kappa = 0.65\%$; and $(129, 10.7)\,\mu\text{m}$ for $\kappa = 2\%$. From the measurement of the coherence length, the horizontal beam size is inferred using directly the VCZ theorem and agrees within the error bar with the theoretical values provided with LOCO. However, along the vertical direction we have experimental evidence that the VCZ theorem cannot be applied and yields to incorrect results. We have performed simulations to support this conclusion, as well as to provide a more reliable relation between the vertical beam size and the transverse coherence length. A simple model yields to $\sigma_y = (8.1 \pm 0.7)\,\mu\text{m}$ for $\kappa = 0.65\%$ and $\sigma_y = (12.5 \pm 1.6)\,\mu\text{m}$ for $\kappa = 2\%$, which provides a better agreement with the theoretical values. Further effects, like the finite length ($\sim 2\text{m}$) of the source point are still to be carefully evaluated.

ACKNOWLEDGEMENTS

REFERENCES

[1] U. Iriso and F. Pérez, "Synchrotron Radiation Monitors at ALBA", in *Proc. EPAC'06*, Edinburgh, UK, Jun. 2006, paper THPLS056, pp. 3410–3412.

[2] L. Torino, U. Iriso, and T. M. Mitsuhashi, "Beam Size Measurements using Synchrotron Radiation Interferometry at ALBA", in *Proc. IBIC'14*, Monterey, CA, USA, Sep. 2014, paper TUPF23, pp. 374–379.

[3] L. Torino and U. Iriso, "Transverse beam profile reconstruction using synchrotron radiation interferometry", *Phys. Rev. Accel. Beams*, vol. 19, pp. 122801, Aug. 2016. doi: 10.1103/PhysRevAccelBeams.19.122801

[4] M. Giglio, M. Carpineti, and A. Vailati, "Space intensity correlations in the near field of the scattered light: a direct measurement of the density correlation function $g(r)$", *Phys. Rev. Lett.*, vol. 85, pp. 1416, Aug. 2000. doi:10.1103/PhysRevLett.85.1416

[5] S. Mazzoni *et al.*, "SODI-COLLOID: a combination of static and dynamic light scattering on board the International Space Station", *Rev. Sci. Instrum.*, vol. 84, pp. 043704, Apr. 2013. doi:10.1063/1.4801852

[6] R. Cerbino *et al.*, "X-ray-scattering information obtained from near-field speckle", *Nat. Phys.*, vol. 4, pp. 238–243, Jan. 2008. doi:10.1038/nphys837

[7] M. D. Alaimo *et al.*, "Probing the transverse coherence of an undulator X-ray beam using brownian nanoparticles", *Phys. Rev. Lett.*, vol. 103, pp. 194805, Nov. 2009. doi:10.1103/PhysRevLett.103.194805

[8] M. Siano *et al.*, "Transverse Beam Size Diagnostics using Brownian Nanoparticles at ALBA", in *Proc. IBIC'16*, Barcelona, Spain, Sep. 2016, pp. 248–252. doi:10.18429/JACoW-IBIC2016-MOPG73

[9] M. Siano *et al.*, "Characterizing temporal coherence of visible synchrotron radiation with heterodyne near field speckles", *Phys. Rev. Accel. Beam*, vol. 20, pp. 110702, Nov. 2017. doi:10.1103/PhysRevAccelBeams.20.110702

[10] S. Mazzoni *et al.*, "Progress on Transverse Beam Profile Measurement Using the Heterodyne Near Field Speckles Method at ALBA", in *Proc. IBIC'18*, Shanghai, China, Sep. 2018, pp. 538–541. doi:10.18429/JACoW-IBIC2018-THOA03

[11] J. W. Goodman, *Statistical Optics*, Wiley-Interscience, New York, 2000.

[12] L. Mandel and E. Wolf, *Optical Coherence and Quantum Optics*, Cambridge University Press, New York, 1995.

[13] G. Benedetti, D. Einfeld, Z. Marti, M. Munoz, "LOCO in the Alba Storage Ring", in *Proc. IPAC'11*, San Sebastian, Spain, Sep. 2011, paper WEPC024, pp. 2055–2057.

[14] G. Geloni, E. Saldin, E. Schneidmiller, and M. Yurkov, "Transverse coherence properties of X-ray beams in third-generation synchrotron radiation sources", *Nucl. Instrum. Methods Phys. Res., Sect. A*, vol. 588, pp. 463-493, Apr. 2018. doi:10.1016/j.nima.2008.01.089